Water Science & Technology

IWA PUBLISHING

Water Science & Technology Vol 86 No 5, 894 doi: 10.2166/wst.2022.252

Competition adsorption of malachite green and rhodamine B on polyethylene and polyvinyl chloride microplastics in aqueous environment

Yiping Zhong[a], Kangkang Wang[b], Changyan Guo[b], Yuli Kou[b], Afaq Hassan[b], Yi Lu[b,*], Jide Wang[b] and Wei Wang[c]

[a] College of Chemistry, Xinjiang University, Urumqi 830046, China
[b] School of Chemical Engineering and Technology, Xinjiang University, Urumqi 830046, China
[c] Department of Chemistry, University of Bergen, Realfagbygget 41, Bergen 5007, Norway
*Corresponding author. E-mail: luyi_xjzjy@163.com

ABSTRACT

Microplastics (MPs) will cause compound pollution by combining with organic pollutants in the aqueous environment. It is important for environmental protection to study the adsorption mechanism of different MPs for pollutants. In this study, the adsorption behaviors of malachite green (MG) and rhodamine B (RhB) on polyethylene (PE) and polyvinyl chloride (PVC) were studied in single systems and binary systems, separately. The results show that in single system, the adsorptions of between MPs for pollutants (MG and RhB) are more consistent with the pseudo-second-order kinetics and Freundlich isotherm model, the adsorption capacity of both MPs for MG is greater than that of RhB. The adsorption capacities of MG and RhB were 7.68 mg/g and 2.83 mg/g for PVC, 4.52 mg/g and 1.27 mg/g for PE. In the binary system, there exist competitive adsorption between MG and RhB on MPs. And the adsorption capacities of PVC for the two dyes are stronger than those of PE. This is attributed to the strong halogen-hydrogen bond between the two dyes and PVC, and the larger specific surface area of PVC. This study revealed the interaction and competitive adsorption mechanism between binary dyes and MPs, which is of great significance for understanding the interactions between dyes and MPs in the multi-component systems.

Key words: competitive adsorption, dyes, mechanism, microplastics

HIGHLIGHTS

- The adsorptions of MG and RhB on PE and PVC are multilayer adsorption.
- The adsorption relationship between two similar types of dyes on different microplastics was investigated.
- PVC has a better adsorption effect because it interacts with two dyes to create halogen-hydrogen bond.
- In the binary system, MG and RhB are competitive.

GRAPHICAL ABSTRACT

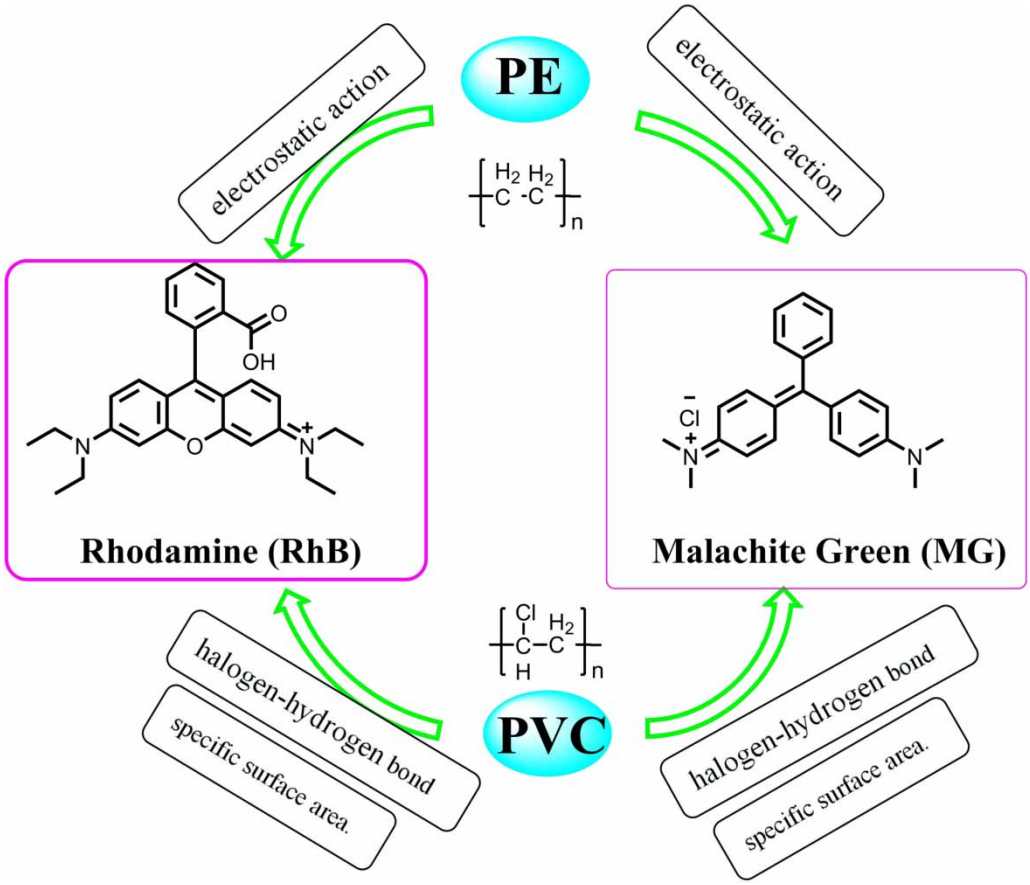

1. INTRODUCTION

It is estimated that by 2050, 1.2×10^9 tons of plastic waste will be released into the natural environment (You *et al.* 2021). Waste plastics will be further degraded or broken up by physical, chemical, and biological processes (Wang *et al.* 2020b; Yang *et al.* 2021). Plastics less than 5 mm in diameter are usually defined as micro-plastics (MPs) (Wang *et al.* 2019). MPs are dispersed in an aqueous environment by the movement of water (Nematollahi *et al.* 2021). MPs are highly susceptible to ingestion by aquatic organisms, causing a variety of adverse effects such as reduced feeding and inflammation (Wang *et al.* 2020a). Therefore, the environment pollution caused by MPs is a major concern for scientists and the public (Qi *et al.* 2021; Ding *et al.* 2020).

Due to their small size, large specific surface area (Fang *et al.* 2019), strong hydrophobicity, and the presence of different functional groups (Cui *et al.* 2022), MPs become carriers of various pollutants (Lv *et al.* 2019; Zhang *et al.* 2019), such as heavy metals (Zhou *et al.* 2019) polycyclic aromatic hydrocarbons (Fang *et al.* 2019), and pesticides (Wang *et al.* 2020c). In an aquatic environment, contaminated MPs are taken up by surrounding aquatic organisms and then transferred through the food chain (Li *et al.* 2021b). Contaminated MPs can release contaminants when they enter organisms, which will cause dual toxicity (Zhang *et al.* 2021), such as low growth rate and reproductive complications (Fu *et al.* 2022), or in more severe cases, the death of the organism. Therefore, the studies of the interaction between contaminants and MPs in the multicomponent systems would be an important research focus nowadays and in future.

Available studies have shown that the capacity and mechanism of the pollutant adsorption on MPs mainly depends on the structure and nature of the polyvinyl chloride (PVC), polyethylene (PE), polypropylene and triclosan (Sheng *et al.* 2020). Currently, PE and PVC are two commonly used plastics (Wu *et al.* 2020; Yu *et al.* 2020b; Chen *et al.* 2021). The adsorption capacity and mechanism of pollutants on MPs with different group may be quite different. Mo *et al.* found that intermolecular van der Waals forces were one of the main adsorption mechanisms for the adsorption of two pesticides by PE (Mo *et al.*

2021). Li *et al.* revealed that the adsorption of three pesticides by PE was mainly physical and controlled by intermolecular van der Waals forces and micro-porous filling mechanisms (Li *et al.* 2021a). Bao *et al.* found that the adsorption of anthracene and its hydroxyl derivatives by PVC was mainly due to electrostatic interactions and CH-π interaction forces (Bao *et al.* 2021a). Wu *et al.*'s study on the adsorption of five kinds of bisphenol A on PVC showed that electrostatic interactions and non-covalent bonding (hydrogen and halogen bonding) were present in the adsorption process (Wu *et al.* 2019b).

Like pesticides, dyes are a large group of contaminants that pose a significant safety risk to humans (Akpan & Hameed 2009). For instance, malachite green (MG) (Bulut *et al.* 2008) is a common methylated di-amino tri-phenyl-methane dye, and Rhodamine B (RhB) (Chatterjee *et al.* 2019) is a highly water-soluble cationic heteroanthracene dye, both of which are highly toxic and carcinogenic in nature (Tariq *et al.* 2020). These two dyes are widely used in the textile, paper, cotton, and dyeing industries and generate large amounts of dye effluent in the environment (Chatterjee *et al.* 2019). However, the studies on their sorption behavior by MPs are very limited.

There are many dyes and MPs in the water system, and many complex multi-component systems are formed. The inevitable interaction between dyes and MPs will lead to more complex environmental behavior. Although Lin *et al.* (2020) explored the interaction mechanism and optimal conditions for nylon plastic to adsorb MG, and You *et al.* explored and found that the aging PE had a better adsorption effect on methylene blue compared with the original plastic (You *et al.* 2021). The adsorption of single dyes on MPs is not enough to explain the real situation in the environment. Thus, at the preliminary stage, the researches on the adsorption relationship of binary component dyes on MPs will be a closer step to the real environment, so it is more meaningful to study the adsorption mechanism of adsorption of MPs with different polarities and dyes in the binary component system.

In this paper, the adsorption kinetics and isotherms of MG and RhB on PE and PVC in single system were investigated. The effect of the salinity and pH on the adsorption behavior for the dyes was studied. On the basis of these results, the competitive adsorptions of the two dyes on MPs were investigated with different ratio of dyes, and possible competitive adsorption mechanisms were proposed. This study would provide a new way for understanding the interactions between dyes and MPs in the multicomponent systems.

2. MATERIALS AND METHODS

2.1. Materials and reagents

Malachite green (MG, A.R. grade), rhodamine B (RhB, A.R. grade), calcium chloride ($CaCl_2$, 96%), 0.1 mol L^{-1} hydrochloric acid (HCl) and sodium hydroxide (NaOH) analytical standard solution were all purchased from Shanghai Aladdin Biochemical Technology Co., Ltd. Sodium chloride (NaCl, A.R. grade) was purchased from Sinopharm Chemical Reagent Co., Ltd. (Shanghai, China). These reagents can be used without further purification. PE and PVC were purchased from Dongguan Plastic raw materials Factory in China. The octanol-water partition coefficient (Kow) of MG and RhB is shown in Table S5.

2.2. Characterization and analysis methods

The surface morphological of MPs were characterized by scanning electron microscopy (SEM) (S-4800 Hitachi, Tokyo, Japan), Fourier transform infrared (FT-IR) (FT/IR-4100 Jasco Inc., Tokyo, Japan) was performed to identify the dominant functional groups of MPs, the hydrophobicity of MPs was measured by contact angle (JY-82B Kruss DSA), the surface potential values of PE and PVC were measured by zeta potential (ZS90, Malvern Inc., UK) and N_2 adsorption-desorption experiment was carried out to determine the surface area, the pore size distributions and the pore volumes of the MPs. The surface area was calculated using Brunauer-Emmett-Teller (BET) method and pore size distribution was analyzed using Barrett-Joiner-Halenda (BJH) model. The concentration of dye was measured by ultraviolet spectrophotometer (UV-2550, Shimadzu, Japan). (The detection limit of MG and RhB is 0.27 mg/L and 0.51 mg/L, in Fig. S2.)

2.3. Batch adsorption experiment

2.3.1. Experimental step

The adsorptions of MG and RhB on PE and PVC were investigated. There are three parallel samples during the experiment, including a blank group without MPs. In general, 60 mg of adsorbent (PE or PVC) and 60 mL of contaminant solution containing 0.1 mol/L $CaCl_2$ were added to a brown glass centrifuge tube. All adsorption experiments were performed in a thermostatic vibrating chamber at a rate of 160 rpm and 25 °C. The concentration of dye was measured by a UV spectrophotometer.

2.3.2. Adsorption experiments

As for kinetics experiments, 60 mg PE and PVC were added to a 60 mL brown glass bottle with an initial concentration of 10 mg/L MG and 5 mg/L RhB solution, respectively. The solution was taken at 0.5, 1, 3, 7, 12, 24, 35, 48, 58, 69 h after adsorption, 2.5 mL samples were collected each time, and centrifuged with a centrifuge at a speed of 10,000 rpm/min for 5 min, and the supernatant was taken. Finally, the equilibrium concentration of the two dyes was determined by a UV spectrophotometer. According to the results of the kinetics experiment, after 60 h of reaction, the adsorption reached equilibrium. Therefore, we have carried out adsorption isotherm experiments. To ensure the adsorption ratio is in the range of 20–80%, the concentration of MG solution was set as 10, 20, 30, 40, and 50 mg/L, and RhB solution was set as 2, 3, 5, 8, 10 mg/L, while the concentration of PE and PVC was maintaining at 60 mg.

To study the effect of salinity on adsorption behavior, different masses of salinity (0, 3, 6, 12, 24, 36, 48 mg) were added into a 60 mL brown glass bottle with 60 mL MG or RhB solutions and 60 mg PE or PVC. To eliminate the interference of the inner wall of the container on dye adsorption, all experiments included blank space, and only MPs and dye solutions were compared. The experimental process is consistent with the adsorption kinetics mentioned above. After 60 h, samples are collected and MPs are removed by centrifugation before analysis.

As for understanding the effect of pH on adsorption behavior, while other conditions were consistent with the adsorption kinetics experiment, different pH values (2, 4, 6, 8, and 10) were set in the experiment. The following experimental operation is consistent with the above-mentioned experiment. The adsorption behavior of MG and RhB on MPs was investigated. Three groups of MG solutions at 10 mg/L including 10 mg/L, 20 mg/L, and 40 mg/L RhB, three groups of RhB solutions at 5 mg/L including 5 mg/L, 10 mg/L, and 20 mg/L/MG were prepared in the adsorption experiment. After adding sorbents (PE and PVC), six groups of suspensions were shaken at 25 °C in dark. Samples were collected and tested after 60 h.

Calculate the adsorption concentration (q_t, mg/g) Equation (1)

$$q_t = \frac{(C_0 - C_t)V}{m} \tag{1}$$

where C_0 (mg/L) is the initial concentration of dye solution, C_t (mg/L) is the concentration of dye at a certain time (min), and m (g) is the mass of PE and PVC, V (L) is the total volume of the solution.

2.3.3. Adsorption kinetics model

Dynamic data were evaluated by pseudo-first-order (2), pseudo-second-order (3) models, and intra-particle diffusion model (4), which were described by equations respectively:

$$\mathrm{Log}(q_e - q_t) = \mathrm{Log}q_e - K_1 t \tag{2}$$

$$\frac{t}{q_t} = \frac{1}{K_2 q_e} + \frac{t}{q_e} \tag{3}$$

$$q_t = k_p t^{0.5} + x_i \tag{4}$$

where q_e (mg/g) refers to the amount of adsorbent adsorbed after reaching equilibrium, and q_t (mg/g) refers to the amount of adsorbent adsorbed at a certain time (min). K_1 (L/min) and K_2 (g/(mg·min)) are rate constants of pseudo-first-order and pseudo-second-order models respectively. While k_p ($g \cdot mg^{-1} \cdot h^{-0.5}$) is the rate constant of the intra-particle diffusion model; and x_i is a number related to the thickness of the interface.

2.3.4. Adsorption isotherm model

Langmuir (5) and Freundlich (6) models are generally used as linear equations to describe the interaction between adsorbents and pollutants in the equilibrium state. Generally, the Langmuir model is used to represent the energy equally distributed on the surface by chemisorption, and adsorption vacancy is balanced; the Freundlich model mainly describes the adsorption

equilibrium of multiphase adsorption.

$$\frac{c_e}{q_e} = \frac{1}{K_L \cdot q_m} + \frac{c_e}{q_m} \tag{5}$$

$$\mathrm{Log}q_e = \mathrm{Log}K_F + \frac{1}{n}\mathrm{Log}c_e \tag{6}$$

q_e (mg/g) and C_e(mg/g) is the adsorption capacity of pollutants at equilibrium and a certain time (min) respectively, in which q_m (mg/g) is the maximum adsorption capacity of MPs under monolayer adsorption. K_L (L/mg) was the surface adsorption equilibrium constant of the Langmuir model, and the larger K_L was, the stronger the adsorption capacity of the adsorbent was. K_F (L/mg) is the adsorption capacity constant in the Freundlich model. 1/n is a constant dependent on adsorption strength.

3. RESULTS AND DISCUSSION

3.1. Characterization of MPs

The morphology of PE is displayed in Figure 1(a) and 1(b), which exhibits that there are many folds on the surface of polyethylene and the particle shape is irregular. This result is similar to the work of Gomes *et al.*, which confirmed that the morphology of PE was rugged and the surface was wrinkled (Gomes de Aragão Belé *et al.* 2021). In addition, the size of PE is about 40 μm. The morphologies of PVC are displayed in Figure 1(c) and 1(d), which show that the surface of PVC is

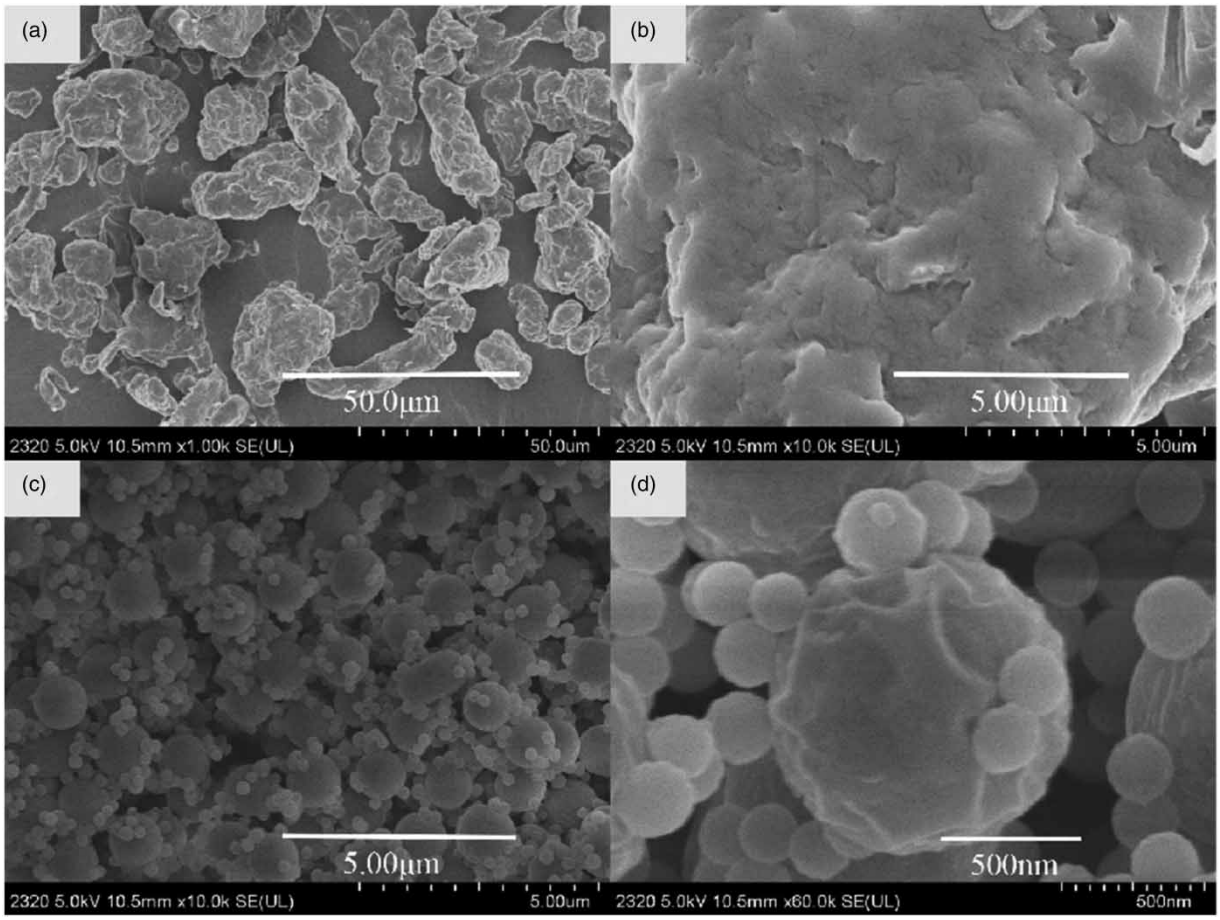

Figure 1 | Scanning electron microscope images of PE (a and b) and PVC (c and d) particles.

relatively smooth and has small holes. The PVC particles, with a size of about 1.2 μm, are spherical and uniform in size. Nguyen *et al.* studied the adsorption of three bivalent metals on PVC. Their results showed that the PVC was also spherical in shape, and displayed a largest surface area than PE (Nguyen *et al.* 2022).

FT-IR spectroscopy was used to characterize the changes of functional groups on PE and PVC surfaces before and after the adsorption of MG and RhB. As shown in Fig. S1(a), the FT-IR spectroscopy of PE before adsorption of dyes shows that the peaks located at 2,920 cm^{-1} and 2,855 cm^{-1} are the stretching vibrations of the C-H bond. The bending vibration and vibration of the C-H bond occurred at 1,465 cm^{-1} and 1,371 cm^{-1}, and 721 cm^{-1}, respectively (You *et al.* 2021; Rozman *et al.* 2021). However, Fig. S1(a) confirmed that no new chemical bonds were formed during the adsorption of PE, which proved that chemical adsorption is not the main factor in the adsorption process (Lin *et al.* 2021).

The FT-IR spectroscopy of PVC before adsorption of dyes is depicted in Fig. S1(b), the peaks located at 2,913 cm^{-1} and 1,427 cm^{-1} correspond to stretching and bending vibrations of -CH_2-. Out-of-plane deformation vibration of Cl-CH at 1,251 cm^{-1} (Ma *et al.* 2019), and the peak of 609 cm^{-1} was attributed to the C-Cl tensile vibration (Bao *et al.* 2021b; Yu *et al.* 2020a). It can be seen from the FT-IR spectrum of Fig. S1(b) that the peaks (1,427 cm^{-1} and 1,251 cm^{-1}) intensities slightly decreased after PVC adsorbed MG (Tang *et al.* 2021a, 2021b). This is the result of the specific interaction between the chlorine groups on PVC and the groups on MG. This confirms that -Cl on PVC will form a halogen-hydrogen bond with the proton-donating functional group of MG to enhance the adsorption (Wu *et al.* 2019b). This halogen-hydrogen bond interaction also exists between PVC and RhB, as can be seen by the green shading in Fig. S1(b), which can be used to predict that PVC would have stronger adsorption capability than that of PE.

Figure 2 shows the N_2 adsorption-desorption isotherms of PE and PVC. The inset of Figure 2(a) and 2(b) shows the pore size distribution curve obtained by the BJH method. The specific surface area (SSA) of MPs will affect the adsorption capacity. The description of microscopic morphology was verified by SSA, as shown in Table S1, which was detected by BET method (Singh *et al.* 2020). The descending order of SSA value of the four MPs with the same particle size was PVC > PE, indicating that the specific surface area of MPs increases with the decrease in particle size (Zhu *et al.* 2021). This result is consistent with the sort of adsorption capacity: PVC > PE.

Zeta potential can be used to describe the surface charge of MPs. It can influence the adsorption of organic pollutants, especially ionized organic pollutants, which are attached to MPs through electron interactions (Wang *et al.* 2022). The surface charge of an adsorbent is closely related to its ability to absorb contaminants. From Figure 3, we can conclude that the point of zero charge (pH_{pzc}) of PE is 4.3 (Xu *et al.* 2018), while pH_{pzc} of PVC is 5.8, and the zeta potential of both PE and PVC toward negative charge from positive charge as the pH increases.

The contact angles of the two MPs are shown in Figure 4, and the result indicates the hydrophilicity and hydrophobicity of the two MPs. The bigger the contact angle of MPs, the stronger the hydrophobicity (Sheng *et al.* 2020). On the contrary, the contact angle is small, the MPs tend to hydrophilicity. In Figure 4(a), the contact angle of PE is 102.58°, while PVC is 90.41° in Figure 4(b), which indicates that the surface of PE is more hydrophobic and PE could absorb hydrophobic dyes easier.

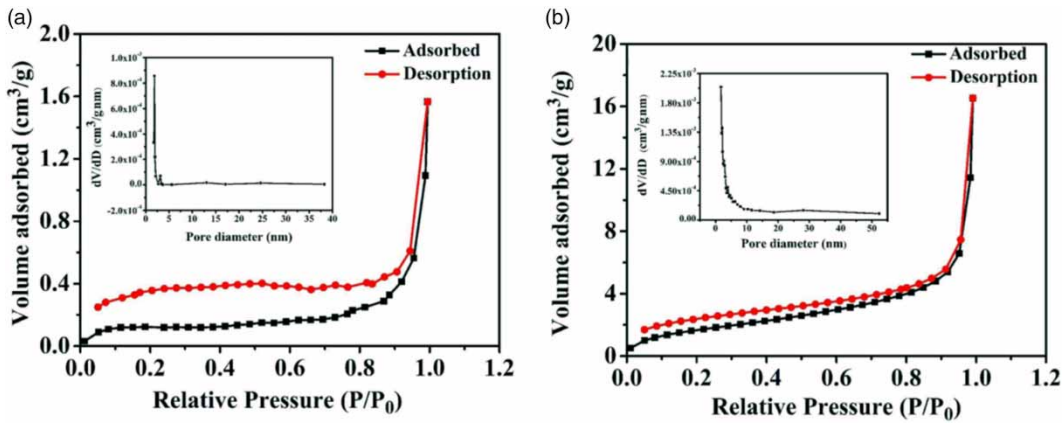

Figure 2 | N_2 adsorption-desorption isotherms; and pore diameter distribution determined by BET method of (a) PE and (b) PVC particles.

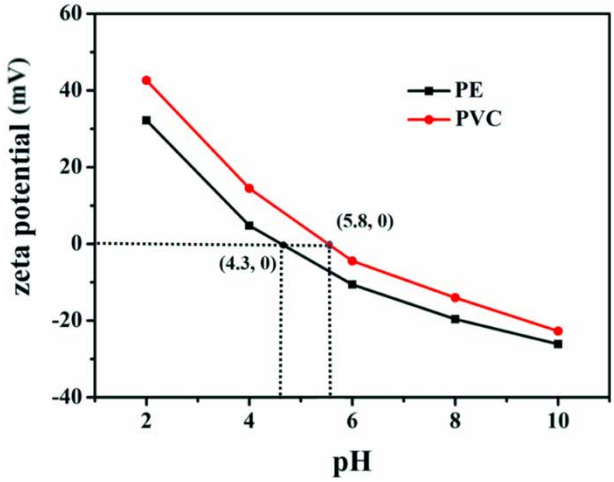

Figure 3 | Zeta potential of PE and PVC under different pH.

3.2. Adsorption kinetics

The adsorption data of RhB and MG on PE and PVC were simulated by using pseudo-first-order, pseudo-second-order, and intra-particle diffusion models. In the initial 20 h, the adsorptions of MG on PE and PVC increased rapidly and the adsorption reactions reached equilibrium after shaking for 60 h as shown in Figure 5(a) and 5(b). From Figure 5(c) and 5(d), the adsorptions of RhB on PE and PVC were also increased rapidly at first and then slows down, and after 60 h the adsorption reactions reached the state of equilibrium. Furthermore, Figure 5(e) illustrates the data fitting results of the intra-particle diffusion model. The results show that the adsorption process is nonlinear and can be divided into three stages, which indicates that the adsorption may be affected by two or more critical stages. The first stage represents the fast reaction stage, which may refer to the attachment of the dyes on the adsorbent surface (Singh *et al.* 2012); the second stage refers to the diffusion of the dye into the pore, showing a slow rate. The third stage is the dynamic equilibrium point. The results are consistent with the results of intra-particle diffusion for the adsorption of norfloxacin on PE (Sun *et al.* 2021). The adsorption of dye on the MPs did not pass through the origin, indicating that the adsorption was not governed by a single diffusion. Therefore, the adsorption process was controlled by a multi-step mechanism (Liu *et al.* 2020b). The kinetic parameters of pseudo-first-order, pseudo-second-order of this work and previous studies investigating dye adsorption on MPs are shown in Table S2 and intra-particle diffusion models for MG and RhB on PE and PVC are shown in Table S3. It can be seen that the dynamic adsorption of two dyes on these two MPs are more consistent with the pseudo-second-order model by the regression coefficient of these three models (Qiongjie *et al.* 2022).

3.3. Adsorption isotherms

Langmuir and Freundlich models were used to simulate the adsorption process of MG and RhB on MPs as shown in Figure 6. The corresponding parameters of the two models were displayed in Table S4. The Langmuir model assumes that the surface

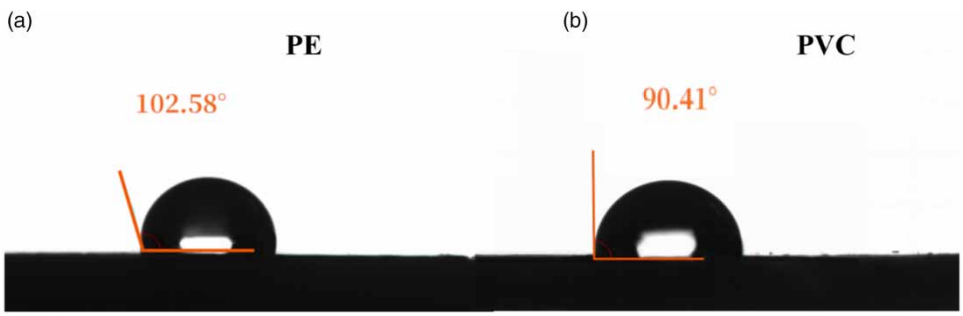

Figure 4 | The contact angles spectra of (a) PE and (b) PVC particles.

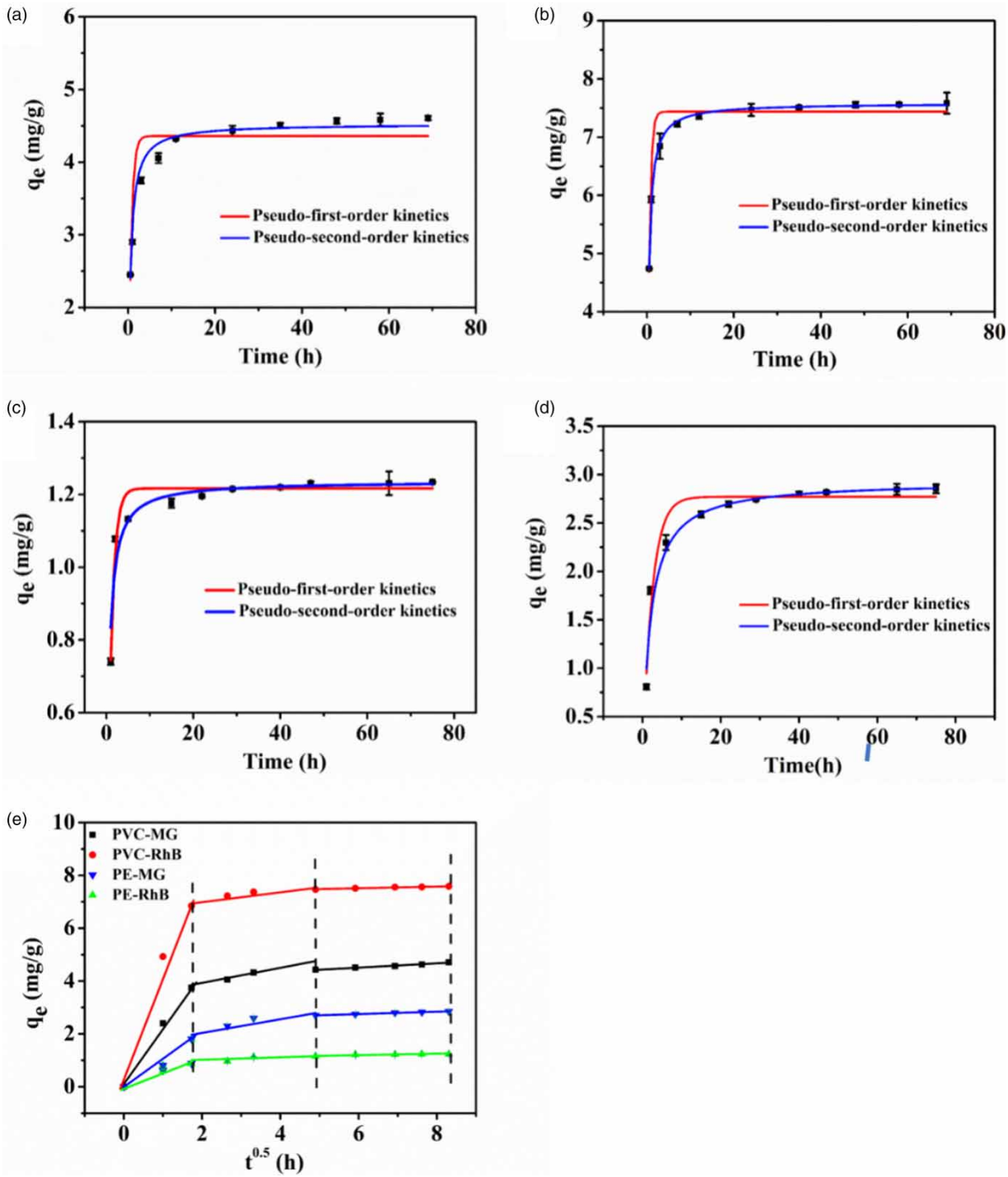

Figure 5 | The pseudo-first- and pseudo-second-order model for MG on PE (a) and PVC (b); for RhB on PE (c) and PVC (d); and the intra-particle diffusion plots for MG and RhB on PE and PVC (PE/PVC: 60 mg; MG: 60 mL and 10 mg/L; RhB: 60 mL and 5 mg/L).

of the adsorbent is uniform with monolayer adsorption of only one molecule per adsorption site (Foo & Hameed 2010). The Freundlich isotherm is the basis of an assumption regarding surface heterogeneity and can be used to model monolayer (chemical adsorption) and multi-layer adsorption (Van der Waals force adsorption) (Yang 1998). The correlation coefficients of Freundlich and Langmuir are slightly different, but as summarized in Table S4, the q_{max} values of the two MPs obtained by the Langmuir equation are far greater than those obtained in our experiments, and the K_L values are tiny, which does not

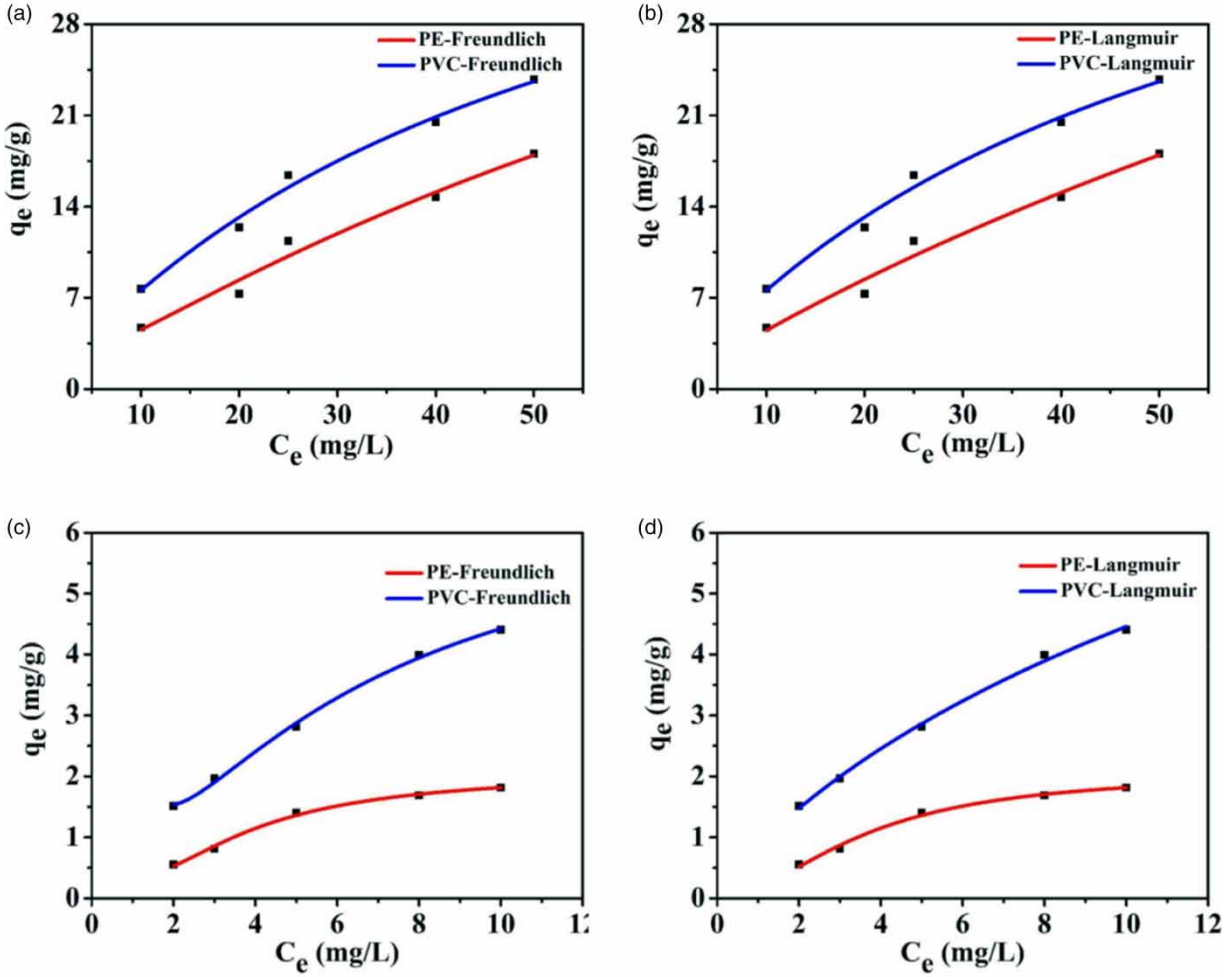

Figure 6 | The Freundlich model of (a) MG and (c) RhB adsorption by MPs, the Langmuir model of (b) MG and (d) RhB adsorption by MPs.

conform to our test results (Zhang *et al.* 2020). Therefore, the Freundlich model is more in line with our experimental results. This phenomenon indicated that all the adsorption of dyes on MPs were multilayer adsorption, rather than molecular adsorption on a uniform surface (Mo *et al.* 2021). This finding is consistent with previous studies on the adsorption of five bisphenol analogs on PVC (Wu *et al.* 2019b). The K_F value is an indicator of adsorption capacity, and the larger the K_F value is, the larger the adsorption capacity is (Liu *et al.* 2020a). In general, PVC is more attractive to bind MG and RhB than PE. In addition, the values of parameter n of Freundlich models deviating significantly from 1 as shown in Table S4, the adsorption process were nonlinear, which means that the distribution of adsorption active sites on PE and PVC could be heterogeneous. The adsorption process involved several adsorption mechanisms (Karimi *et al.* 2019; Koopal *et al.* 2020), such as electrostatic adsorption, surface deposition, etc.

3.4. Effect of pH

In an aqueous environment, pH has an important effect on the adsorption between pollutants (MG and RhB) and MPs. Therefore, the influences of different pH on the adsorptions of MG and RhB on PE and PVC were investigated, as shown in Figure 7. It can be seen that the adsorptions of MG and RhB on MPs gradually increased with the increase of pH. In addition, the adsorption capacities of MG and RhB on two MPs increased slowly when the pH changed from 2 to 6. These experimental results correspond exactly to the pH_{pzc} of PE and PVC (in Figure 3). MG and RhB are cationic dyes and the surface of MPs gradually turns from positive to neutral. When the pH is higher than 4.3 and 5.8, the surfaces of PE and PVC are negative charged. It leads to a gradual increase in the adsorption capacity by electrostatic attraction

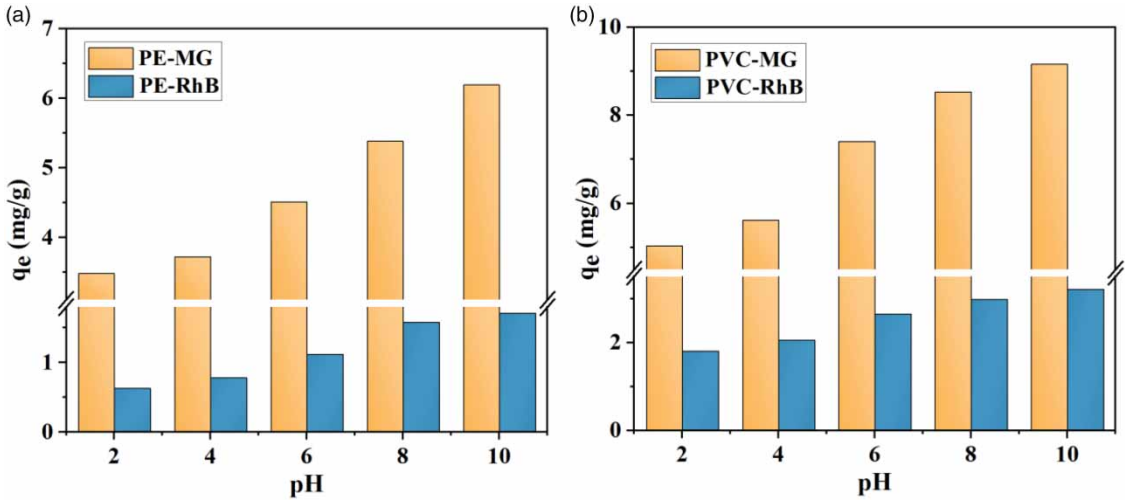

Figure 7 | The influence of pH on the adsorptions of MG and RhB on PE (a) and PVC (b).

(Lin *et al.* 2021). And as pH continues to augment, the electrostatic attraction makes the adsorption capacity continue to increase. These showed that electrostatic action plays an important role in the adsorption process. This is similar to the conclusion of Tang *et al.*, that the high capacity of Pb(II) in high pH solutions may be attributed to electrostatic attraction (Tang *et al.* 2020).

3.5. Effect of salinity

Sodium chloride (NaCl) is the most common salt in the natural environment, and it can significantly affect the adsorption between MPs and pollutants in the water environment. As shown in Figure 8, with the increase of salinity in the system, the adsorption of PE and PVC to these two pollutants decreases. It should be noted that both contaminants (MG and RhB) are stable cationic forms in neutral aqueous solutions, whereas PE and PVC surfaces are both negatively charged when pH > 6 (according to Figure 3). Therefore, it indicates that the introduction of Na^+ weakens the electrostatic attraction between the two pollutants and PE and PVC (Zhao *et al.* 2015).

3.6. Study on the co-adsorption of MG and RhB by MPs

According to the adsorption kinetics of MG and RhB on PE and PVC in single system, the equilibrium adsorption capacities of PVC for MG and RhB are 7.68 and 2.83 mg/g, and the equilibrium adsorption capacities of PE for MG and RhB are 4.52 and 1.27 mg/g, respectively. The adsorption capacities of PVC for MG and RhB are significantly higher than those of PE. In addition, the characterization results show that PVC has more adsorption sites than PE.

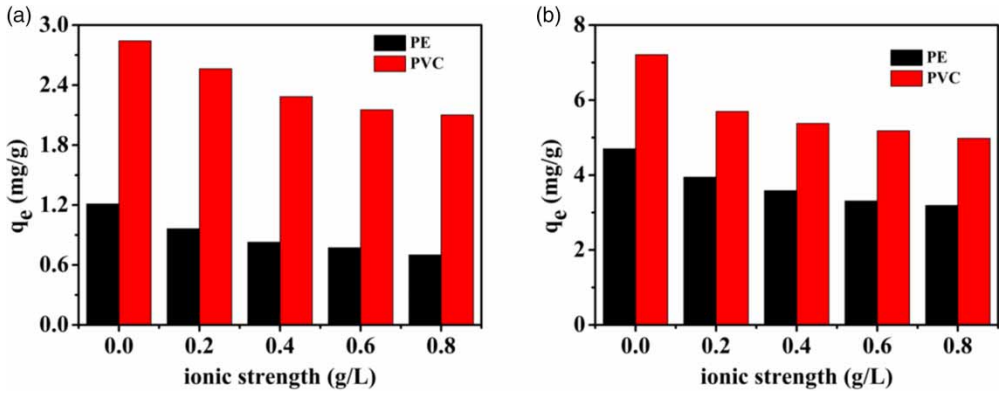

Figure 8 | The effect of ionic concentration (NaCl) on the adsorption of RhB (a) and MG (b) on PE and PVC.

The adsorption difference of pollutants on PE and PVC in binary system was evaluated (when RhB and MG coexist). As shown in Figure 9, the adsorption experiments of the two dye pollutants on PE and PVC at different ratios were carried out, respectively. It can be seen from Figure 9(a), when MG concentration is constant, the adsorption amount of MG on PVC decreases obviously with the increase of RhB/MG ratio, while the adsorption amount of RhB increases. It indicates that the increased RhB occupies the adsorption site on PE or PVC, resulting in a significant decrease in MG adsorption capacity. Similarly, according to Figure 9(c) and 9(d), when RhB concentration remains unchanged, the adsorption capacity of PE or PVC for RhB decreases with the increase of MG/RhB ratio, while the adsorption capacity of MG increases significantly. These two results clearly indicate that MG and RhB compete for adsorption on PE or PVC, and the change of adsorption capacity of the two dyes are caused by the competition for adsorption sites on MPs. These results are consistent with the results of competitive adsorption of Pb (II) and Cd (II) on biochar reported in literature (Ni *et al.* 2019).

In addition, by comparing Figure 9(a) and 9(b), it can be also found that the concentration of MG remains unchanged (10 mg/L). When RhB/MG ratio was 1:1, the adsorption capacity of PE and PVC for RhB/MG is 1.2/2.5 and 1.7/5.6, respectively. When the ratio was 2:1, the adsorption capacity of PE to RhB/MG is 1.7/1.7, the adsorption capacity of PVC to RhB/MG is 2.0/5.1. When the ratio was 4:1, the adsorption capacity of PE to RhB/MG is 2.6/0.8, and the adsorption capacity of PVC to RhB/MG is 3.5/4.1. By comparison, it can be found that under the condition of the same RhB/MG ratio change

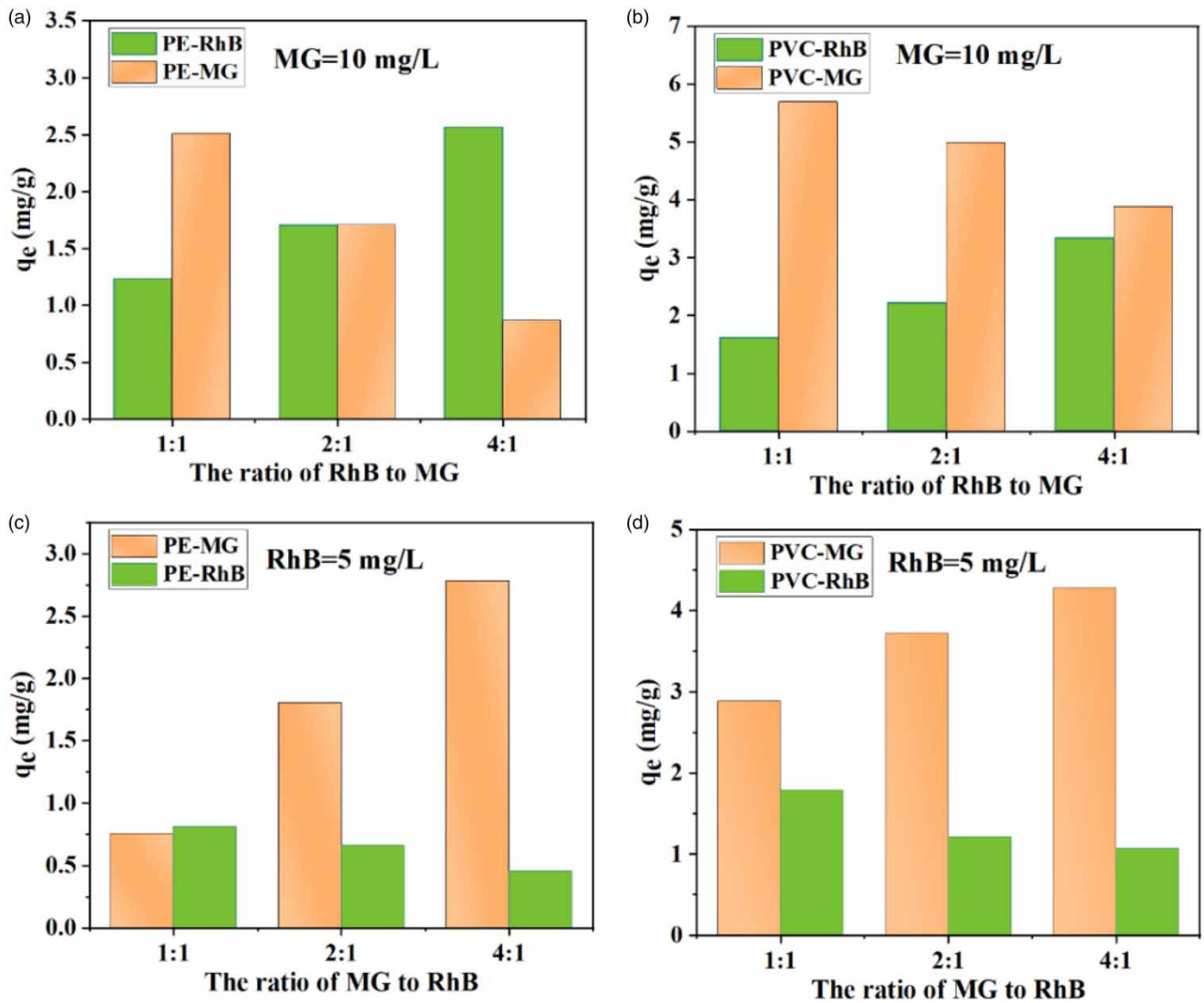

Figure 9 | The adsorption of different ratios of [RhB/MG] on PE (a) and PVC (b) as well as different ratios of [MG/RhB] on PE (c) and PVC (d).

(from 1:1 to 4:1), the change of the adsorption ratio of the two dyes on PE is significantly greater than that on PVC. Similarly, by comparing Figure 9(c) and 9(d), the concentration of RhB remains unchanged, and the MG/RhB ratio increases from 1:1 to 4:1 under the same conditions (increasing from 1:1 to 4:1), the change of adsorption capacity of the two dyes on PE is also significantly greater than that on PVC. This is because PE adsorption for two dyes is mainly electrostatic action, and the SSA of PE is smaller than PVC, so the adsorption site of PE is less than PVC, which indicates PE is susceptible to external adsorption concentration changes. This is consistent with the results that the adsorption capacity of aged PE is higher than that of PE MPs, which attributes to the larger surface area of aged PE MPs (Lan *et al.* 2020). So, with the ratios of two dyes changing, the change of adsorption on PE is obvious. Meanwhile, the hydrophilicity of PVC is stronger than that of PE, it is consistent with the results that the addition of surfactants makes MPs have higher hydrophilicity, which significantly improves the adsorption of lead ions (Shen *et al.* 2020). In addition, the adsorption between PVC with MG and RhB will form halogen-hydrogen bonds resulting in more adsorption sites (Pengfei *et al.* 2018). Hence, PVC has more adsorption sites than PE, and is less affected by the change of the concentration of external adsorbed matter. Therefore, the adsorption mechanism of PE to the two dyes is mainly electrostatic action, while the adsorption of PVC to MG and RhB is controlled by electrostatic action, hydrophilic and hydrophobic, SSA and halogen hydrogen bond.

The results in Figure 9 show that there is competition between MG and RhB in the binary system. This is consistent with the the competitive adsorption between tetracycline and ciprofloxacin on montmorillonite (Wu *et al.* 2019a). The adsorption capacity of two dyes on PVC is greater than that on PE. This may be due to the fact that PVC has a larger SSA than PE, and the ability to form halogen-hydrogen bonds with MG and RhB, which makes PVC have more adsorption sites.

4. CONCLUSION

In this paper, the adsorption behaviors of MG and RhB were investigated over PE and PVC MPs in one- and two-component systems. Following a number of intermittent experiments, we observed that the pseudo-second-order kinetics and the Freundlich isothermal model can accurately explain the adsorption kinetics and isothermal process of two dyes on MPs. The results show that the adsorption processes are multilayer, and the adsorption ability of MG and RhB on PE is lower than that of PVC, and MG exhibits greater adsorption amounts on the two MPs than on RhB. Consequently, the nature of PE and PVC has an influence on the adsorption results. The adsorption of the two dyes on PE is primarily regulated by electrostatic action, while the adsorptions of RhB and MG on PVC are mainly affected by halogen-hydrogen bond and specific surface area. Furthermore, the adsorptions of MG and RhB on PE and PVC exhibited competitive interactions in the dual-dye system. The adsorption amounts of MG on PE and PVC are greater than those of RhB due to the stronger halogen bonding. MG shows a greater adsorption capacity probably because it is more hydrophilic than RhB. This study focuses on competitive adsorption behavior, which provides a new idea for studying the complex adsorption behavior of multi-component dye pollutants on MPs.

ACKNOWLEDGEMENTS

We acknowledged the financial support from the National Natural Science Foundation of China (32061133005), and the Research Council of Norway (RCN, project 320456). This work was also supported by Key Laboratory of Oil and Gas Fine Chemicals, Ministry of Education & Xinjiang Uygur Autonomous Region.

FUNDING

This work was supported by the National Natural Science Foundation of China (32061133005) and the Research Council of Norway (RCN, project 320456).

AUTHOR CONTRIBUTION

Yiping Zhong: Conceptualization, acquisition of data, investigation, validation, analysis and interpretation of data, drafting of the manuscript, visualization. Kangkang Wang: Study conception and design, drafting of the manuscript, data curation, validation, visualization. Changyan Guo: Data curation, validation, visualization. Yuli Kou: Investigation, validation, visualization. Afaq Hassan: Visualization. Yi Lu: Conceptualization, methodology, validation, resources, supervision. Jide Wang: Conceptualization, validation, resources, writing-review & editing, supervision, project administration, funding acquisition. Wei Wang: Data curation, validation, visualization, funding acquisition.

DATA AVAILABILITY STATEMENT

All relevant data are included in the paper or its Supplementary Information.

CONFLICT OF INTEREST

The authors declare there is no conflict.

REFERENCES

Akpan, U. G. & Hameed, B. H. 2009 Parameters affecting the photocatalytic degradation of dyes using TiO2-based photocatalysts: a review. *J. Hazard. Mater.* **170** (2), 520–529.

Bao, Z.-Z., Chen, Z.-F., Lu, S.-Q., Wang, G., Qi, Z. & Cai, Z. 2021a Effects of hydroxyl group content on adsorption and desorption of anthracene and anthrol by polyvinyl chloride microplastics. *Sci. Total Environ.* **790**, 148077.

Bao, Z.-Z., Chen, Z.-F., Zhong, Y., Wang, G., Qi, Z. & Cai, Z. 2021b Adsorption of phenanthrene and its monohydroxy derivatives on polyvinyl chloride microplastics in aqueous solution: model fitting and mechanism analysis. *Sci. Total Environ.* **764**, 142889.

Bulut, E., Özacar, M. & Şengil, İ. A. 2008 Adsorption of malachite green onto bentonite: equilibrium and kinetic studies and process design. *Microporous Mesoporous Mater.* **115** (3), 234–246.

Chatterjee, M. J., Ahamed, S. T., Mitra, M., Kulsi, C., Mondal, A. & Banerjee, D. 2019 Visible-light influenced photocatalytic activity of polyaniline -bismuth selenide composites for the degradation of methyl orange, rhodamine B and malachite green dyes. *Appl. Surf. Sci.* **470**, 472–483.

Chen, Y., Li, J., Wang, F., Yang, H. & Liu, L. 2021 Adsorption of tetracyclines onto polyethylene microplastics: a combined study of experiment and molecular dynamics simulation. *Chemosphere* **265**, 129133.

Cui, R., Jong, M.-C., You, L., Mao, F., Yao, D., Gin, K. Y.-H. & He, Y. 2022 Size-dependent adsorption of waterborne Benzophenone-3 on microplastics and its desorption under simulated gastrointestinal conditions. *Chemosphere* **286**, 131735.

Ding, L., Mao, R., Ma, S., Guo, X. & Zhu, L. 2020 High temperature depended on the ageing mechanism of microplastics under different environmental conditions and its effect on the distribution of organic pollutants. *Water Res.* **174**, 115634.

Fang, S., Yu, W., Li, C., Liu, Y., Qiu, J. & Kong, F. 2019 Adsorption behavior of three triazole fungicides on polystyrene microplastics. *Sci. Total Environ.* **691**, 1119–1126.

Foo, K. Y. & Hameed, B. H. 2010 Insights into the modeling of adsorption isotherm systems. *J. Environ. Chem.* **156** (1), 2–10.

Fu, L., Xi, M., Nicholaus, R., Wang, Z., Wang, X., Kong, F. & Yu, Z. 2022 Behaviors and biochemical responses of macroinvertebrate Corbicula fluminea to polystyrene microplastics. *Sci. Total Environ.* **813**, 152617.

Gomes de Aragão Belé, T., Neves, F., Cristale, T., Prediger, J., Constapel, P., & F, M. & Dantas, R. 2021 Oxidation of microplastics by O3 and O3/H2O2: surface modification and adsorption capacity. *J. Water Process Eng.* **41**, 102072.

Karimi, S., Tavakkoli Yaraki, M. & Karri, R. R. 2019 A comprehensive review of the adsorption mechanisms and factors influencing the adsorption process from the perspective of bioethanol dehydration. *Renewable Sustainable Energy Rev.* **107**, 535–553.

Koopal, L., Tan, W. & Avena, M. 2020 Equilibrium mono- and multicomponent adsorption models: from homogeneous ideal to heterogeneous non-ideal binding. *Adv. Colloid Interface Sci.* **280**, 102138.

Lan, T., Wang, T., Cao, F., Yu, C., Chu, Q. & Wang, F. 2020 A comparative study on the adsorption behavior of pesticides by pristine and aged microplastics from agricultural polyethylene soil films. *Ecotoxicol. Environ. Saf.* **209**, 111781.

Li, H., Wang, F., Li, J., Deng, S. & Zhang, S. 2021a Adsorption of three pesticides on polyethylene microplastics in aqueous solutions: kinetics, isotherms, thermodynamics, and molecular dynamics simulation. *Chemosphere* **264**, 128556.

Li, W., Pan, Z., Xu, J., Liu, Q., Zou, Q., Lin, H. & Huang, H. 2021b Microplastics in a pelagic dolphinfish (Coryphaena hippurus) from the Eastern Pacific Ocean and the implications for fish health. *Sci. Total Environ.* **809**, 151126.

Lin, L., Tang, S., Wang, X., Sun, X. & Yu, A. 2020 Adsorption of malachite green from aqueous solution by nylon microplastics: reaction mechanism and the optimum conditions by response surface methodology. *Process Saf. Environ. Prot.* **140**, 339–347.

Lin, L., Tang, S., Wang, X., Sun, X. & Yu, A. 2021 Hexabromocyclododecane alters malachite green and lead(II) adsorption behaviors onto polystyrene microplastics: interaction mechanism and competitive effect. *Chemosphere* **265**, 129079.

Liu, Y., Huang, Y., Zhang, C., Li, W., Chen, C., Zhang, Z. & Zhang, Y. 2020a Nano-FeS incorporated into stable lignin hydrogel: a novel strategy for cadmium removal from soil. *Environ. Pollut.* **264**, 114739.

Liu, Z., Qin, Q., Hu, Z., Yan, L., Ieong, U.-I. & Xu, Y. 2020b Adsorption of chlorophenols on polyethylene terephthalate microplastics from aqueous environments: kinetics, mechanisms and influencing factors. *Environ. Pollut.* **265**, 114926.

Lv, L., Qu, J., Yu, Z., Chen, D., Zhou, C., Hong, P. & Li, C. 2019 A simple method for detecting and quantifying microplastics utilizing fluorescent dyes – Safranine T, fluorescein isophosphate, Nile red based on thermal expansion and contraction property. *Environ. Pollut.* **255**, 113283.

Ma, J., Zhao, J., Zhu, Z., Li, L. & Yu, F. 2019 Effect of microplastic size on the adsorption behavior and mechanism of triclosan on polyvinyl chloride. *Environ. Pollut.* **254**, 113104.

Mo, Q., Yang, X., Wang, J., Xu, H., Li, W., Fan, Q. & Zhang, Y. 2021 Adsorption mechanism of two pesticides on polyethylene and polypropylene microplastics: DFT calculations and particle size effects. *Environ. Pollut.* **291**, 118120.

Nematollahi, M. J., Keshavarzi, B., Mohit, F., Moore, F. & Busquets, R. 2021 Microplastic occurrence in urban and industrial soils of Ahvaz metropolis: a city with a sustained record of air pollution. *Sci. Total Environ.* **819**, 152051.

Nguyen, T.-B., Ho, T.-B.-C., Huang, C. P., Chen, C.-W., Chen, W.-H., Hsieh, S. & Dong, C.-D. 2022 Adsorption of lead(II) onto PE microplastics as a function of particle size: influencing factors and adsorption mechanism. *Chemosphere* **304**, 135276.

Ni, B.-J., Huang, Q.-S., Wang, C., Ni, T.-Y., Sun, J. & Wei, W. 2019 Competitive adsorption of heavy metals in aqueous solution onto biochar derived from anaerobically digested sludge. *Chemosphere* **219**, 351–357.

Pengfei, W., Zongwei, C., Hangbiao, J. & Yuanyuan, T. 2018 Adsorption mechanisms of five bisphenol analogues on PVC microplastics. *Sci. Total Environ.* **09**, 049.

Qi, K., Lu, N., Zhang, S., Wang, W., Wang, Z. & Guan, J. 2021 Uptake of Pb(II) onto microplastic-associated biofilms in freshwater: adsorption and combined toxicity in comparison to natural solid substrates. *J. Hazard. Mater.* **411**, 125115.

Qiongjie, W., Yong, Z., Yangyang, Z., Zhouqi, L., Jinxiaoxue, W. & Huijuan, C. 2022 Effects of biofilm on metal adsorption behavior and microbial community of microplastics. *J. Hazard. Mater.* **424**, 127340.

Rozman, U., Turk, T., Skalar, T., Zupančič, M., Čelan Korošin, N., Marinšek, M. & Kalčíková, G. 2021 An extensive characterization of various environmentally relevant microplastics – material properties, leaching and ecotoxicity testing. *Sci. Total Environ.* **773**, 145576.

Shen, M., Song, B., Zeng, G., Zhang, Y., Teng, F. & Zhou, C. 2020 Surfactant changes lead adsorption behaviors and mechanisms on microplastics. *Chem. Eng. J.* **405**, 126989.

Sheng, C., Zhang, S. & Zhang, Y. 2020 The influence of different polymer types of microplastics on adsorption, accumulation, and toxicity of triclosan in zebrafish. *J. Hazard. Mater.* **402**, 123733.

Singh, S. K., Townsend, T. G., Mazyck, D. & Boyer, T. H. 2012 Equilibrium and intra-particle diffusion of stabilized landfill leachate onto micro- and meso-porous activated carbon. *Water Res.* **46** (2), 491–499.

Singh, N., Khandelwal, N., Tiwari, E., Naskar, N., Lahiri, S., Lützenkirchen, J. & Darbha, G. K. 2020 Interaction of metal oxide nanoparticles with microplastics: impact of weathering under riverine conditions. *Water Res.* **189**, 116622.

Sun, M., Yang, Y., Huang, M., Fu, S., Hao, Y., Hu, S. & Zhao, L. 2021 Adsorption behaviors and mechanisms of antibiotic norfloxacin on degradable and nondegradable microplastics. *Sci. Total Environ.* **807** (3), 151042.

Tang, S., Lin, L., Wang, X., Feng, A. & Yu, A. 2020 Pb(II) uptake onto nylon microplastics: interaction mechanism and adsorption performance. *J. Hazard. Mater.* **386**, 121960.

Tang, S., Lin, L., Wang, X., Sun, X. & Yu, A. 2021a Adsorption of fulvic acid onto polyamide 6 microplastics: influencing factors, kinetics modeling, site energy distribution and interaction mechanisms. *Chemosphere* **272**, 129638.

Tang, Y., Liu, Y., Chen, Y., Zhang, W., Zhao, J., He, S. & Yang, Z. 2021b A review: research progress on microplastic pollutants in aquatic environments. *Sci. Total Environ.* **766**, 142572.

Tariq, M., Muhammad, M., Khan, J., Raziq, A., Uddin, M. K., Niaz, A. & Rahim, A. 2020 Removal of Rhodamine B dye from aqueous solutions using photo-Fenton processes and novel Ni-Cu@MWCNTs photocatalyst. *J. Mol. Liq.* **312**, 113399.

Wang, J., Liu, X., Liu, G., Zhang, Z., Wu, H., Cui, B. & Zhang, W. 2019 Size effect of polystyrene microplastics on sorption of phenanthrene and nitrobenzene. *Ecotoxicol. Environ. Saf.* **173**, 331–338.

Wang, F., Gao, J., Zhai, W., Liu, D., Zhou, Z. & Wang, P. 2020a The influence of polyethylene microplastics on pesticide residue and degradation in the aquatic environment. *J. Hazard. Mater.* **394**, 122517.

Wang, Q., Zhang, Y., Wangjin, X., Wang, Y., Meng, G. & Chen, Y. 2020b The adsorption behavior of metals in aqueous solution by microplastics effected by UV radiation. *J. Environ. Sci.* **87**, 272–280.

Wang, T., Yu, C., Chu, Q., Wang, F., Lan, T. & Wang, J. 2020c Adsorption behavior and mechanism of five pesticides on microplastics from agricultural polyethylene films. *Chemosphere* **244**, 125491.

Wang, X., Zhang, R., Li, Z. & Yan, B. 2022 Adsorption properties and influencing factors of Cu(II) on polystyrene and polyethylene terephthalate microplastics in seawater. *Sci. Total Environ.* **812**, 152573.

Wu, M., Zhao, S., Jing, R., Shao, Y., Liu, X., Lv, F. & Liu, A. 2019a Competitive adsorption of antibiotic tetracycline and ciprofloxacin on montmorillonite. *Appl. Clay Sci.* **180**, 105175.

Wu, P., Cai, Z., Jin, H. & Tang, Y. 2019b Adsorption mechanisms of five bisphenol analogues on PVC microplastics. *Sci. Total Environ.* **650**, 671–678.

Wu, J., Xu, P., Chen, Q., Ma, D., Ge, W., Jiang, T. & Chai, C. 2020 Effects of polymer aging on sorption of 2,2′,4,4′-tetrabromodiphenyl ether by polystyrene microplastics. *Chemosphere* **253**, 126706.

Xu, B., Liu, F., Brookes, P. C. & Xu, J. 2018 The sorption kinetics and isotherms of sulfamethoxazole with polyethylene microplastics. *Mar. Pollut. Bull.* **131**, 191–196.

Yang, C.-h. 1998 Statistical mechanical study on the freundlich isotherm equation. *J. Colloid Interface Sci.* **208** (2), 379–387.

Yang, L., Zhang, Y., Kang, S., Wang, Z. & Wu, C. 2021 Microplastics in freshwater sediment: a review on methods, occurrence, and sources. *Sci. Total Environ.* **754**, 141948.

You, H., Huang, B., Cao, C., Liu, X., Sun, X., Xiao, L. & Chen, Q. 2021 Adsorption–desorption behavior of methylene blue onto aged polyethylene microplastics in aqueous environments. *Mar. Pollut. Bull.* **167**, 112287.

Yu, F., Li, Y., Huang, G., Yang, C., Chen, C., Zhou, T. & Ma, J. 2020a Adsorption behavior of the antibiotic levofloxacin on microplastics in the presence of different heavy metals in an aqueous solution. *Chemosphere* **260**, 127650.

Yu, F., Yang, C., Huang, G., Zhou, T., Zhao, Y. & Ma, J. 2020b Interfacial interaction between diverse microplastics and tetracycline by adsorption in an aqueous solution. *Sci. Total Environ.* **721**, 137729.

Zhang, X., Zheng, M., Yin, X., Wang, L., Lou, Y., Qu, L. & Qiu, Y. 2019 Sorption of 3,6-dibromocarbazole and 1,3,6,8-tetrabromocarbazole by microplastics. *Mar. Pollut. Bull.* **138**, 458–463.

Zhang, J., Chen, H., He, H., Cheng, X., Ma, T., Hu, J. & Zhang, L. 2020 Adsorption behavior and mechanism of 9-Nitroanthracene on typical microplastics in aqueous solutions. *Chemosphere* **245**, 125628.

Zhang, L., Li, Y., Wang, W., Zhang, W., Zuo, Q., Abdelkader, A. & Kim, K.-H. 2021 The potential of microplastics as adsorbents of sodium dodecyl benzene sulfonate and chromium in an aqueous environment. *Environ. Res.* **197**, 111057.

Zhao, Y., Gu, X., Li, S., Han, R. & Wang, G. 2015 Insights into tetracycline adsorption onto kaolinite and montmorillonite: experiments and modeling. *Environ. Sci. Pollut. Res.* **22** (21), 17031–17040.

Zhou, Y., Liu, X. & Wang, J. 2019 Characterization of microplastics and the association of heavy metals with microplastics in suburban soil of central China. *Sci. Total Environ.* **694**, 133798.

Zhu, Y., Li, X., Wang, L. & Chen, F. 2021 Adsorption of BDE-209 to polyethylene microplastics: effect of microplastics property and metal ions. *Water Air Soil Pollut*. **232**, 494.

First received 9 April 2022; accepted in revised form 5 August 2022. Available online 16 August 2022